EurJOC
European Journal of Organic Chemistry

Research Article
doi.org/10.1002/ejoc.202400753

Chemistry Europe
European Chemical Societies Publishing

www.eurjoc.org

S-Aryl Substitution Enhances Acidity of the 1,2,4-Triazolium Scaffold

Matthew S. Smith,[a] Toby J. Blundell,[a] Ian Hickson,[b] and AnnMarie C. O'Donoghue*[a]

The 1,2,4-triazolium scaffold in asymmetric organocatalysis results in remarkable rate accelerations, with reactions typically occurring via *N*-heterocyclic carbene (NHC) intermediates. Although the most acidic NHC pre-catalyst class, there remains scope for further increases in acidity particularly for aqueous organocatalysis applications. The acidity-enhancing effects of thio-substituents on carbon acidity are well-documented but not explored in the 1,2,4-triazolium scaffold. Herein, we report the synthesis of a large series of *N*, *N*-dialkyl-C(3)-*S*-aryltriazolium ions and quantitative kinetic evaluation of C(5)-H acidity. The direct attachment of *S*-aryl substituents to the triazolium heterocycle results in substantial increases in protofugalities (kinetic acidities) with second order rate constants (k_{DO}) for C(5)-H deprotonation by DO^- base that are 2.9–60.3 fold higher than for reference 1,4-dimethyl-1,2,4-triazolium iodide in D_2O solution. Protofugalities for the *N*, *N*-dialkyl-C(3)-*S*-aryltriazolium series are similar to commonly used bicyclic *N*-aryl-1,2,4-triazolium organocatalysts despite having two electron donating *N*-alkyl substituents. This highlights the future potential of this NHC design which could enable the introduction of two chiral alkyl substituents close to the C(5) carbenic position with pre-catalyst acidity controlled by distal C(3)-*S*-aryl substitution. Detailed X-ray structural data-protofugality correlations enabled evaluation of the *S*-aryl substituent effect origins. C(5)-H pK_a values (16.9–18.6) were calculated by utilisation of experimental protofugalities.

Introduction

N-heterocyclic carbenes (NHCs) have diverse applications in many areas ranging from catalysis to materials science.[1] For most applications, NHCs are generated through *in situ* deprotonation of a conjugate acid heterocyclic azolium salt (Scheme 1a). Many heterocyclic frameworks may be employed, and the 1,2,4-triazolium scaffold (**1**, X = Y = N) is arguably the most widely applied NHC pre-catalyst in organocatalysis.[1d] Triazolium pre-catalysts provide access to a broad range of transformations and product architectures under relatively mild reaction conditions. In recent years, the chemistry accessible by triazolium-derived catalysis has been extended from classical nucleophilic catalysis by acyl-anion-like chemistry to a range of radical mediated processes.[2] The focus of contemporary NHC organocatalysis has also shifted towards more sustainable solvent media such as water.[3]

Inspiration for the field of NHC organocatalysis stemmed from the mechanism of action of thiazolium-derived cofactor, Thiamin **2** (Scheme 1b).[4] This sulfur-containing azolium salt is a cofactor for a broad range of enzymatic transformations, such as C–C bond formation and cleavage reactions.[5] Initial efforts to emulate this chemistry in organocatalysis focused on

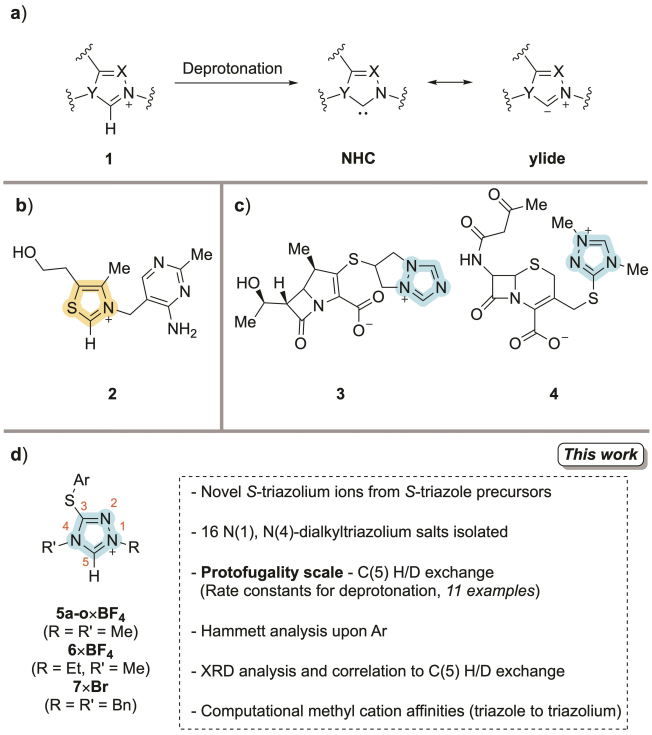

Scheme 1. a) Deprotonation of heterocyclic azolium salt **1** to give *N*-heterocyclic carbenes (NHCs). b) Structure of Thiamin **2** (Vitamin B1). c) Examples of 1,2,4-triazolium-containing compounds **3** and **4** with antibacterial activities. d) This work on 3-*S*-aryl-1,2,4-triazolium salts.

[a] *M. S. Smith, T. J. Blundell, A. C. O'Donoghue*
Department of Chemistry, Durham University, Lower Mount Joy, South Rd, Durham DH1 3LE, United Kingdom
E-mail: annmarie.odonoghue@durham.ac.uk

[b] *I. Hickson*
Cancer Research Horizons Therapeutic Innovation, Newcastle University Centre for Cancer, Translational and Clinical Research Institute, Faculty of Medical Sciences, Newcastle University, Newcastle Upon Tyne NE2 4HH, United Kingdom

Supporting information for this article is available on the WWW under https://doi.org/10.1002/ejoc.202400753

Research Article
doi.org/10.1002/ejoc.202400753

modifications of the thiazolium scaffold and subsequently moved to an exploration of alternative heterocyclic scaffolds.[5e–g] The 1,2,4-triazolium salts have delivered success in asymmetric NHC organocatalysis in part owing to increased pre-catalyst acidity from three nitrogen heteroatoms, but also an increased propensity towards modification close to the carbenic position. 1,2,4-Triazolium-containing molecules also have extensive applications beyond organocatalysis including as anticancer, antibacterial and antifungal agents in medicinal chemistry (*e.g.* antibacterial agent, Biapenem **3**, Scheme 1c).[6]

Despite the widespread applications of 1,2,4-triazolium species in catalysis, there has been limited exploration of *S*-substituted triazolium ions. For effective organocatalysis in water it has been recognised that the field can benefit from improvements in catalyst design including towards increased (pre)catalyst acidities.[1b] Most NHC pre-catalysts have pK_as higher than water thus would benefit from acidity-enhancing substituents. The increase in carbon acidity by sulfur-substitution is well-documented particularly in the case of α-sulfur substituents.[7] Whilst there are several examples of 1,2,4-triazolium compounds of medicinal chemistry relevance with direct *S*-alkyl substitution at C(3) (*e.g.* cephalosporin scaffold **4**,[8] Scheme 1c), there are no *S*-aryl examples to our knowledge.

Herein we report the synthesis and kinetic evaluation of a large series of *S*-aryl substituted 1,2,4-triazolium salts (Scheme 1d). 29 novel triazolium salts have been isolated as part of this work, with kinetic analysis of C(5)-H/D exchange by ^{1}H NMR spectroscopy enabling construction of a protofugality scale[9–10] and Hammett analysis. Protofugalities, or rate constants for C(5)-H deprotonation, underpin NHC generation and catalytic applications. By obtaining X-ray diffraction (XRD) data for ten triazolium salts, correlations between protofugalities and solid-state structural parameters allow for the origins of the *S*-aryl substituent effect to be probed.

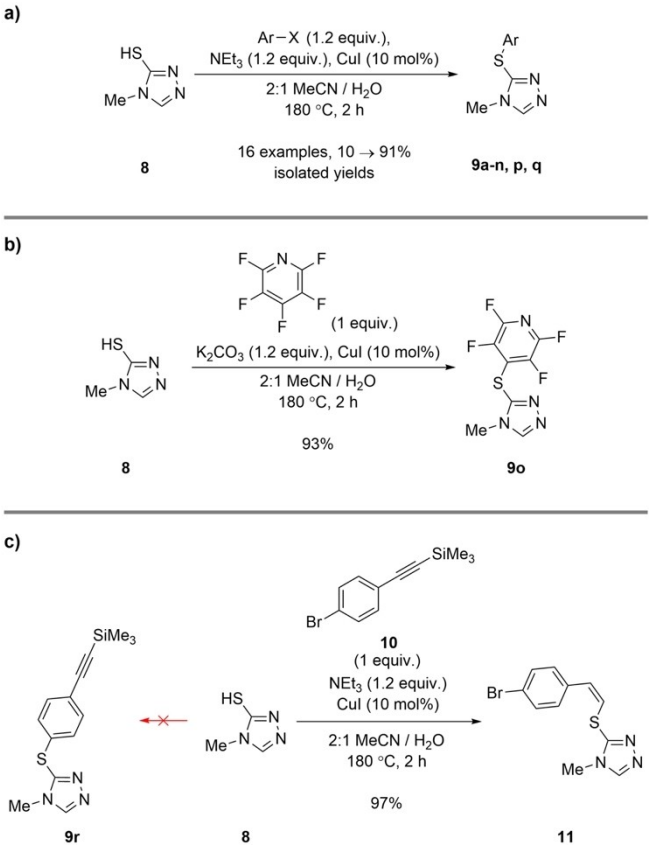

Scheme 2. Overview of 3-*S*-aryltriazole syntheses undertaken within this work. a) General synthesis of *S*-triazoles **9a-n**, **9p** and **9q** by microwave-assisted Ullmann coupling. b) Synthesis of the 2,3,5,6-tetrafluoropyrid-4-yl analogue *S*-triazole **9o**. c) Attempted Ullmann coupling of **8** with a protected phenylacetylene led to ethenyl-conjugated *S*-triazole **11** in high yields.

Results and Discussion

Synthesis of *S*-aryltriazolium Salts

N, *N*-dialkyl *S*-aryltriazolium salts were accessed by initial formation of neutral *S*-aryl triazoles (Scheme 2) followed by *N*-alkylation to cationic triazolium tetrafluoroborate salts (Scheme 3). The *S*-aryl triazoles were prepared from commercially available 4-methyl-4*H*-1,2,4-triazole-3-thiol **8** by Ullmann coupling to a series of aryl iodides. Initial experiments explored the coupling of iodobenzene to thiol **8** in the presence of a range of bases in acetone, acetonitrile and dimethylformamide solvents (ESI, Table S1). The best results (81% isolated yield **9a**) were obtained using triethylamine in a 2:1 acetonitrile:water mixture with microwave heating to 180 °C for 2 h (Scheme 2a and Table 1).

Using these conditions, the substrate scope was extended to a range of aryl iodides (Scheme 2a) allowing for the isolation of 15 *S*-aryl triazoles **9a-n**, **9p** and **9q** in moderate to excellent yields (Table 1). In addition, coupling of thiol **8** and pentafluoropyridine (PFP) in the presence of potassium carbonate (Scheme 2b) provided access to *S*-triazole (**9o**). The preparation of 4-ethynyl substituted *S*-triazole **9r** was also explored using trimethylsilyl-protected 4-bromophenylacetylene **10** (Scheme 2c). Unexpectedly, stereoselective addition to give the ethenyl-conjugated *S*-triazole **11** was instead observed in very high yields. Attempted Ullmann coupling using 4-bromophenylacetylene in place of **10** similarly gave addition product **11** (82% yield) rather than the desired product of *S*-aryl coupling. For six *S*-aryltriazoles, single crystal XRD structural analysis could be performed (ESI, Figure S1, Section S1.3). The *S*-triazoles are seen to adopt a roughly perpendicular arrangement of aryl and triazolyl rings, with slipped-stack packing of the aryl rings.

N, *N*-dialkyl *S*-aryltriazolium salts were then prepared by *N*-methylation of *S*-aryl triazoles using trimethyloxonium tetrafluoroborate (Scheme 3a). The desired 1,4-dimethyl-3-(arylthio)triazolium salts **5a-o·BF$_4$** were the major products in all cases, verified by single crystal XRD (ESI, Figure S2 and Section S1.4). ^{1}H NMR data could be additionally used to distinguish **5a-o·BF$_4$** from the isomeric 2,4-dimethyl-3-(arylthio)triazolium salts **12a-o·BF$_4$** as the ^{1}H NMR C(5)-H chemical shift values for the desired 1,4-isomer are ~0.7–1 ppm higher than for the 2,4-isomer in $CDCl_3$ and DMSO-d^6. Furthermore, the isolated regioisomer could be distinguished

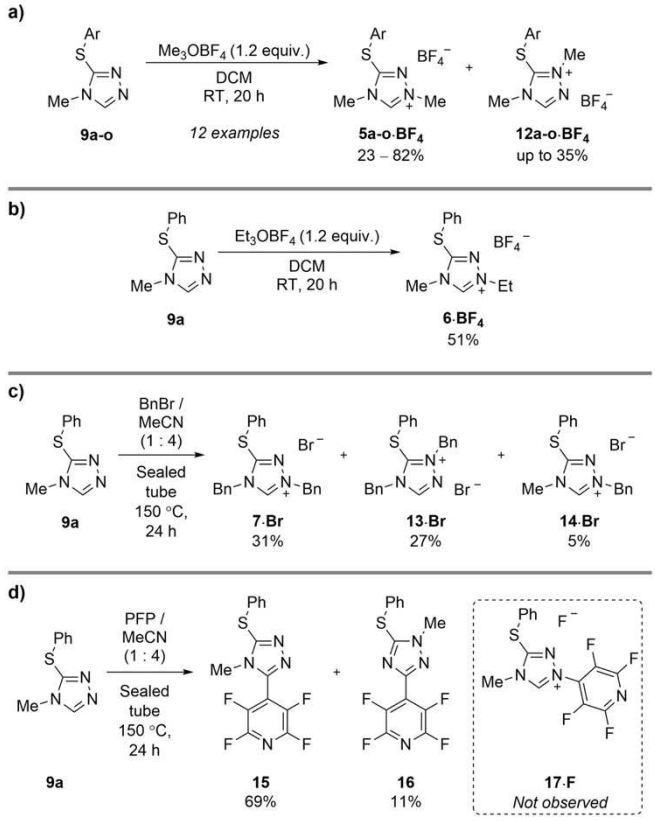

Scheme 3. Overview of 3-*S*-aryl-1,2,4-triazolium salt syntheses undertaken within this work. a) *N*-Methylation of **9a**-**o** was used to access 1,4-dialkyl-*S*-triazolium salts (**5a**-**o**·BF_4) and 2,4-dialkyl-*S*-triazolium salts (**12a**-**o**·BF_4). b) *N*-Ethylation of **9a** led to **6**·BF_4. c) Using excess benzyl bromide, dibenzylated *S*-triazolium salts **7·Br** and **13·Br** were isolated as major products. d) The reaction of PFP with **9a** gave C(5)-substituted *S*-phenyltriazoles.

by differing hydrogen exchange rates in protic deuterated solvents (*vide infra*, ESI Section S3.5). Attempted *N*-methylation of **11** gave a complex mixture and was not further pursued.

Other alkylating and arylating agents were also explored in reactions with the *S*-phenyl triazole **9a**. Triethyloxonium tetrafluoroborate was used to access 1-ethyl-4-methyl-3-(phenylthio)triazolium salt **6**·BF_4 (Scheme 3b). The lower isolated yield was owing to the formation of a more complex product mixture attributed to alkyl exchange under the reaction conditions (ESI, Section S1.1.3). Use of excess benzyl bromide under forcing conditions (Scheme 3c) resulted in the formation of the *N, N*-dibenzyl *S*-triazolium salts **7·Br** and **13·Br** as the major isolated products. This was presumed to result from the onward reaction of initially formed 1-benzyl-4-methyl *S*-triazolium salt **14·Br** which was only isolated in 5% yield under these conditions. The yields of all *N*, *N*-dialkyl triazolium salts are listed in Table 1.

With isolation of both regioisomers in the majority of cases, the selectivity of *N*-alkylation could be investigated. Selectivities of 80% or greater towards formation of 1,4-dialkyltriazolium product were achieved in the methylation of *S*-aryltriazoles bearing *para*-substitution on the *S*-aryl ring. The introduction of bulky *ortho*-substituents led to significantly decreased selectivity in methylation likely owing to the out-of-plane arrangement for the *S*-aryl ring facilitating access to both N(1) and N(2). The forcing conditions involved in the benzylation of **9a** potentially account for the lack of selectivity observed between **7·Br** and **13·Br**.

Density functional theory (DFT) calculations with the 'Estimating Nucleophilicity and Electrophilicity' (EsNuEl) application[11] were undertaken using r^2SCAN-3c SMD(DMSO) single-point calculations on previously optimised lowest energy conformers for each compound (ESI, Section S2). When considering nucleophilicity, EsNuEl computes Methyl Cation Affinities (MCAs) that consider the addition of the methyl cation to each atom within the molecule (Equation 1). Differences in MCA values are reported in Table 1. In agreement with experimental observations, the calculations show a preference for N(1)-methylation of *S*-triazoles, with MCA values for addition at N(2) between 0.4 and 10.8 kJ mol^{-1} less than at N(1) (Table 1).

$$\mathrm{Nuc} + \mathrm{CH_3^+} \xrightarrow{\Delta E} \text{MCA product} \qquad \mathrm{MCA} \equiv -\Delta E \qquad (1)$$

XRD analysis provided access to structural data for ten *S*-aryltriazolium salts (ESI, Figure S2 and Section S1.4, CCDC 2366204–2366212, 2366219). The out-of-plane conformation of the *S*-aryl and triazolyl rings observed for *S*-aryltriazoles is conserved in the triazolium salts.

N-Arylation under a wide range of conditions showed limited success, with the most promising conditions involving the use of copper catalysts with diamine ligands (ESI, Section S1.5). The reaction of PFP with **9a** led to an unexpected byproduct whereby the C(5)-H is exchanged for a 2,4,5,6-tetrafluoropyrid-4-yl (TFP) substituent (Scheme 3d). It is proposed that the desired *S*-triazolium **17·F** is an intermediate in the reaction pathway to **15** and **16**, however clear evidence for the existence of **17·F** was not obtained (ESI, Section S1.6). XRD analysis was possible for **15**, showing a 55° dihedral angle between the triazolyl and tetrafluoropyrid-4-yl rings (ESI, Section S1.6).

Kinetic Evaluation of Proton Transfer

We have previously determined rate constants for deprotonation (protofugalities) of a broad range of 1,2,4-triazolium salts.[12] Hydrogen/deuterium exchange is commonly applied to quantitatively assess the kinetic lability of protons attached to carbon, which is important for catalytic applications.[13] For low concentrations of the C(5)-protonated triazolium salts in D_2O solution, the exchange of the acidic C(5)-H for deuterium is irreversible, and there is good evidence to support a stepwise H/D exchange mechanism via an *N*-heterocyclic carbene (NHC) intermediate under these conditions.[12d,13e,g] As NHC reprotonation/deuteration is known to be fast with a rate constant close to that for dielectric relaxation of solvent, the overall observed rate of H/D exchange may be equated with rate-limiting deprotonation to form the solvent equilibrated carbene.

Using the same approach (Scheme 4), first and second order rate constants for exchange of the C(5)-H of 1,4-dialkyl *S*-

Research Article
doi.org/10.1002/ejoc.202400753

Chemistry Europe
European Chemical Societies Publishing

Table 1. Synthetic yields of *S*-aryl triazoles and dialkyltriazolium salts (isolated yields unless stated otherwise) and computational Methyl Cation Affinities.

R	Ar	Yield –*S*-Aryl triazole (%)	Yield – 1,4-dialkyltriazolium (%)	Yield – 2,4-dialkyltriazolium (%)	ΔMCA (N(1)→N(2))[a] (kJ mol^{-1})
Me	Ph	**9a**, 81	**5a·BF$_4$**, 82	**12a·BF$_4$**, 2[b]	−5.66
Me	*p*-OMe-Ph	**9b**, 29[c]	**5b·BF$_4$**, 80	**12b·BF$_4$**, 10	−5.20
Me	2,6-Me-Ph	**9c**, 72	**5c·BF$_4$**, 44	**12c·BF$_4$**, 35	−5.65
Me	*p*-^{t}Bu-Ph	**9d**, 40	**5d·BF$_4$**, 35	**12d·BF$_4$**, 7	−4.95
Me	*p*-Me-Ph	**9e**, 60	**5e·BF$_4$**, 47	**12e·BF$_4$**, 3	−4.87
Me	*p*-F-Ph	**9f**, 78	**5f·BF$_4$**[d]	**12f·BF$_4$**[d]	−7.77
Me	*p*-I-Ph	**9g**, 40	**5g·BF$_4$**, 55	**12g·BF$_4$**, 4	−6.15
Me	*p*-Br-Ph	**9h**, 75	**5h·BF$_4$**, 51	**12h·BF$_4$**, 1	−6.59
Me	*p*-CHO-Ph	**9i**, 16	**5i·BF$_4$**, 72[e]	**12i·BF$_4$**, 13[c]	−8.40
Me	*p*-COOMe-Ph	**9j**, 21	**5j·BF$_4$**, 63	**12j·BF$_4$**, 5	−8.68
Me	*p*-COMe-Ph	**9k**, 10	**5k·BF$_4$**, 68	**12k·BF$_4$**, 9	−8.14
Me	*p*-CF_3-Ph	**9l**, 69	**5l·BF$_4$**[d]	**12l·BF$_4$**[d]	−9.17
Me	*p*-CN-Ph	**9m**, 12	**5m·BF$_4$**, 23	**12m·BF$_4$**, 5	−7.40
Me	*p*-NO_2-Ph	**9n**, 91	**5n·BF$_4$**, 77	**12n·BF$_4$**, 5	−10.76
Me	TFP[f]	**9o**, 93	**5o·BF$_4$**, 53	**12o·BF$_4$**, 1	−8.97
Me	*p*-COOH-Ph	**9p**, 97[g]	-[h]	-[h]	−8.39[i]
Me	Pyrid-2-yl	**9q**, 61	-[j]	-[j]	−0.38[i]
Me	CH=CH-(*p*-Br–Ph)	**11**, 97	-[j]	-[j]	−10.31[i]
Et	Ph	**9a**, 81	**6·BF$_4$**, 51[k]	-[l]	−5.66
Bn	Ph	**9a**, 81	**7·Br**, 31 **18·Br**, 5	**13·Br**, 27	−5.66

[a] Difference in calculated methyl cation affinity (ΔMCA = MCA(N(2)) - MCA(N(1))) between N(1)-methylation and N(2)-methylation of the *S*-aryl triazoles determined using the EsNuEl application (Equation 1). [b] NMR conversion. Minor product in crude ^{1}H NMR spectrum but could not be isolated and purified. LC–MS retention time also consistent with minor isomer. [c] Aryl bromide used rather than aryl iodide. [d] Synthesis not attempted. [e] NMR conversion. Major product in crude ^{1}H NMR spectrum but could not be isolated and purified. LC–MS retention time also consistent with major isomer. [f] TFP = Tetrafluoropyrid-4-yl. [g] NMR conversion and not isolated. [h] Preferential methylation of carboxylic acid substituent rather than triazole. [i] ΔMCA (N(1)→N(2)) calculated for comparison although other methylation sites available. [j] Reaction attempted but complex mixture observed. [k] Yield with 1 equivalent Et_3OBF_4. [l] Complex mixture owing to alkyl rearrangement under reaction conditions (ESI Section 1.1.3).

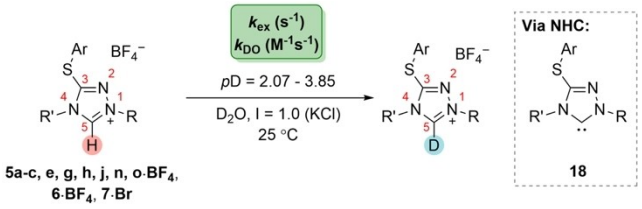

Scheme 4. C(5)-H/D-exchange of *S*-aryl-1,2,4-triazolium salts monitored by ^{1}H NMR spectroscopy; NHC **18** is formed as intermediate in a stepwise H/D-exchange mechanism with consecutive deprotonation and reprotonation steps.

aryltriazolium salts for deuterium were determined for eleven examples in solutions of DCl or deuterated formate buffers in D_2O, at 25 °C and ionic strength = 1.0 (KCl). Apart from **7·Br**, where solubility issues were observed, all *S*-triazolium salts were investigated within fully aqueous conditions; kinetic analysis of **7·Br** necessitated the addition of 20 v% MeCN-d^3 to the D_2O solution. Experiments were undertaken at known p*D* values, allowing for the calculation of deuteroxide concentration (ESI Section S3.1). As observed previously for other triazolium salts,[12] C(5)-H/D exchange above p*D* 4 was too fast for kinetic monitoring by ^{1}H NMR spectroscopy for all *S*-triazolium salts explored.

To ensure accuracy of NMR signal quantification, T_1 values for the C(5)-hydrogens of the *S*-aryltriazolium salts were determined in 0.1 M DCl solution in D_2O (p*D* 1) using the inversion recovery method (ESI, Section S3.2). All *S*-triazolium salts have half-lives for H/D-exchange significantly longer than the inversion recovery experiment (~15 min) under these conditions. Table 2 summarises the T_1 values obtained for **5a-o·BF$_4$**, **6·BF$_4$**, and **7·Br** which range from 3.0–6.5 seconds. For **5a·BF$_4$** with the largest T_1 = 6.5 s at p*D* 1, a closely similar value was also obtained at p*D* 2 (T_1 = 6.7 s). An upper value of T_1 (C(5)-H) = 7 s was assumed and an overall relaxation delay of 35 s (5 × T_1) was employed for this study (ESI, Section S3.2).

In all cases, H/D-exchange was the only reaction evident and no parallel reactions such as hydrolytic ring opening, or demethylation were observed under these dilute aqueous conditions at low p*D*. As a result, the overall H/D-exchange process for *S*-aryltriazolium salts was cleanly pseudo first order in dilute aqueous solution. The pseudo first-order rate constants for the exchange process, k_{ex} (s^{-1}), were determined from the slope of semilogarithmic plots of the fraction of remaining

Research Article
doi.org/10.1002/ejoc.202400753

Table 2. Summary of data obtained in the kinetic evaluation of *S*-triazolium salts.

Analogue	T_1 (s) [a]	k_{DO} ($M^{-1}s^{-1}$) [b]	Log_{10} k_{DO}	σ_X [c]
5a·BF_4	6.51	4.25 (±0.03)×10^7	7.63	0.00
5b·BF_4	5.67	2.70 (±0.07)×10^7	7.43	−0.27
5c·BF_4	4.49	2.16 (±0.13)×10^7	7.33	−0.25[d]
5e·BF_4	5.56	3.27 (±0.03)×10^7	7.51	−0.17
5g·BF_4	5.67	4.60 (±0.05)×10^7	7.82	+0.18
5h·BF_4	4.86	4.43 (±0.02)×10^7	7.65	+0.23
5j·BF_4	5.75	6.61 (±0.13)×10^7	7.82	+0.45
5n·BF_4	6.25	9.20 (±0.36)×10^7	7.96	+0.78
5o·BF_4	5.90	1.62 (±0.04)×10^8	8.21	+1.22[d]
6·BF_4	4.97	3.38 (±0.03)×10^7	7.53	-[e]
7·Br	3.00	4.51 (±0.10)×10^8	8.65	-[e]

[a] T_1 values determined in 0.1 M DCl in D_2O using the inversion recovery method. [b] k_{DO} values obtained using Equation 4. [c] Hammett $\sigma_{p\text{-}X}$ taken from Hansch *et al.*[14] [d] σ_x calculated as described in ESI Section S3.4. [e] Not included in Hammett analysis.

substrate, f(s) versus time (Equations 2 and 3). In Equation 2, I(t) and I(0) are the peak integrals at time 't' and zero for the signal owing to the C(5)-H of the *S*-aryltriazolium salts integrated relative to internal standard. Figure 1a shows representative semilogarithmic plots of ln f(s) versus time for the H/D-exchange reaction of **5a·BF_4** at different p*D* values. Representative NMR overlays, additional plots of f(s) or ln f(s) versus time, all results of kinetic fitting and tabulated values of k_{ex} are provided in the ESI (Section S3.3).

$$f(s) = \frac{I(t)}{I(0)} \quad (2)$$

$$\ln f(s) = -k_{ex}t \quad (3)$$

$$k_{ex} = k_{DO}[DO^-] \quad (4)$$

$$\log_{10}k_{ex} = \log_{10}\left(\frac{k_{DO}K_w}{\gamma_{DO}}\right) + pD \quad (5)$$

Using k_{ex} values determined at different p*D*s the second-order rate constant, k_{DO} ($M^{-1}s^{-1}$), was then obtained for each *S*-triazolium salt using Equations 4 and 5 where $K_w = 10^{-14.87}$ M^2 is the ion product of D_2O at 25 °C[15] and γ_{DO} is the apparent activity coefficient of deuteroxide under our experimental conditions (ESI, Section S3.1.4). Figure 1b shows a representative plot of k_{ex} versus deuteroxide concentration according to Equation 4. The excellent linear correlation supports a first order dependence on DO^-. The slope of unity for plots of Log_{10} k_{ex} against p*D*, corresponding to Equation 5, similarly confirm a first order dependence of the H/D-exchange rate upon DO^- concentration. The second-order rate constant, k_{DO} ($M^{-1}s^{-1}$), is then obtained from the slope or y-axis intercept when fitting to Equations 4 or 5, respectively.

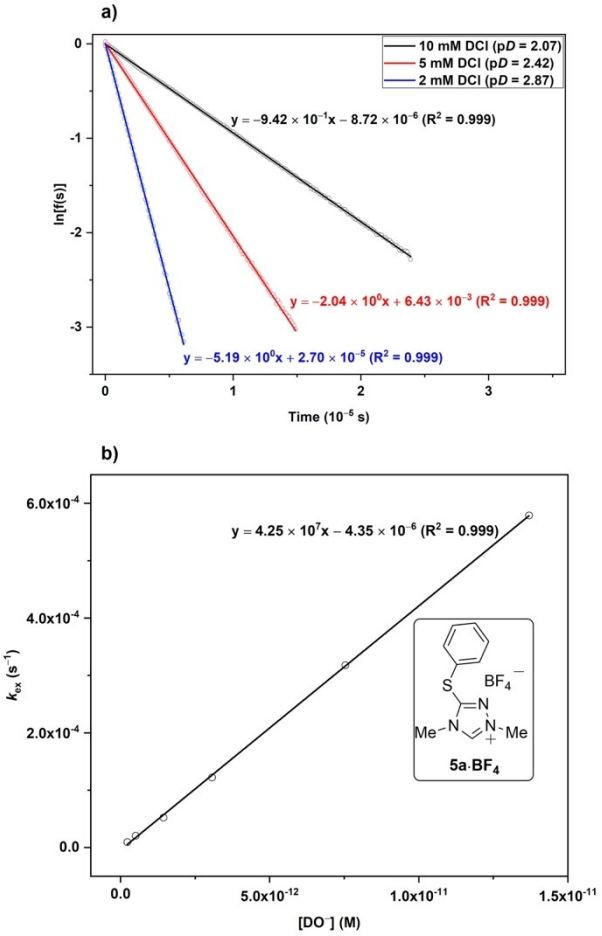

Figure 1. a) Semilogarithmic plots of the fraction of remaining substrate as a function of time for **5a·BF_4** to determine the pseudo first-order rate constant k_{ex} (s^{-1}) at each p*D*; b) Plot of k_{ex} (s^{-1}) against DO^- concentration (M) for **5a·BF_4** to determine the second-order rate constant for C(5)-deprotonation, k_{DO} ($M^{-1}s^{-1}$).

Table 2 summarises k_{DO} and Log_{10} k_{DO} values obtained within this work from fitting to Equation 4. Values obtained from fitting to Equations 4 or 5 (ESI Section 3.3) are closely similar in all cases except for **5c·BF_4** where a variance >0.13 was observed likely owing to the limited number of data points. The comparison of reactivities towards deprotonation by deuteroxide anion, k_{DO}, allows for a comparison of kinetic acidities, or protofugalities. In this case, the common base DO^- is the conjugate base of solvent water thus the rate constants are relevant to all applications of *S*-triazolium salts in aqueous media.

Figure 2 includes a Protofugality Scale which facilitates comparisons of Log_{10} k_{DO} values for all C(3)-*S*-aryltriazolium salts (Table 2) and previous data for a range of triazolium and imidazolium conjugate acids of NHCs.[12d,16–17] Relative to 1,4-dimethyltriazolium iodide **19**,[16] all of the *S*-aryltriazolium ions **5a-o·BF_4**, **6·BF_4** and **7·Br** have significantly higher protofugalities by up to ~2 orders of magnitude (ΔLog_{10} k_{DO} = 0.5 to 1.8) demonstrating the acidifying effect of the introduction of an *S*-aryl substituent at C(3). Electron-withdrawing substituents upon the *S*-aryl ring increase the protofugality, whilst electron

Research Article
doi.org/10.1002/ejoc.202400753

Chemistry Europe
European Chemical Societies Publishing

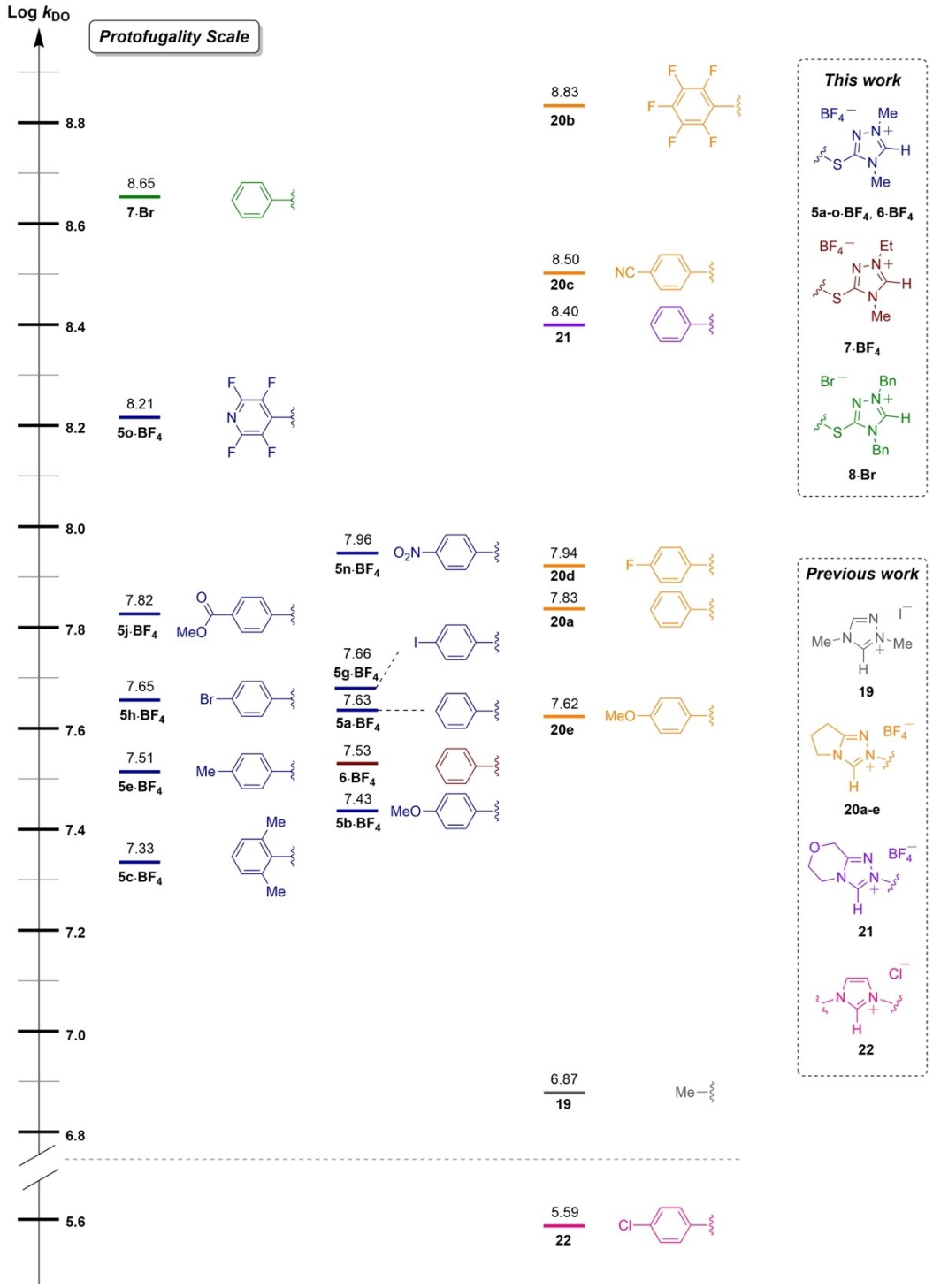

Figure 2. Protofugality scale for the *S*-triazolium salts analysed in this work. Representative k_{DO} values from previous NHC proton transfer studies are also included: 1,4-dimethyl-1,2,4-triazolium iodide **19**,[16] pyrrolidine-fused triazolium salts **20a-e**,[12d] morpholine-fused triazolium salts **21**,[12d] and imidazolium salt **22**.[17]

donating substituents lower k_{DO} relative to *S*-phenyl analogue **5a·BF$_4$**. For example, changing the aryl substituent from *p*-methyl (**5e·BF$_4$**) to *p*-methoxycarbonyl (**5j·BF$_4$**) increases Log_{10} k_{DO} by 0.32 corresponding to a 2-fold increase in k_{DO}. The introduction of an *N*-ethyl substituent in place of one of the *N*-methyl groups (**6·BF$_4$**) shows a minimal change in k_{DO} (c.f. **5a·BF$_4$**). Overall, dibenzyl triazolium **7·Br** has the highest k_{DO} value of the compounds analysed in this work. In general, electron withdrawing substituents destabilise the cationic conjugate acid relative to the formally neutral NHC, which favours deprotonation and increases protofugality.

Importantly, the acidifying effect of an *S*-aryl substituent at C(3) results in **5 a-o·BF$_4$**, **6·BF$_4$** and **7·Br** having similar protofugalities overall to commonly used *N*-aryl 1,2,4-triazolium organocatalysts (**20 a-e**, **21**)[13a–d] despite the former having two electron donating *N*-alkyl substituents that typically decrease protofugality. This highlights the potential of the *S*-aryl scaffold for introducing two stereogenic *N*-alkyl substituents close to the carbenic position whilst maintaining kinetic acidity, whereas widely applied *N*-aryl scaffolds (**20 a-e**, **21**) only permit chiral modification on one side via the fused ring component. Finally, the protofugalities of all triazolium salts are substantially higher than bis-*N*-arylimidazolium salts (e. g. **22**) owing to the presence of an additional electron withdrawing nitrogen in the NHC ring.

Hammett analysis of the *S*-triazolium protofugality data was then performed using σ-values for the *S*-aryl substituents (Table 2 and ESI Section S3.4). Good linear correlations were observed with and without the inclusion of data for substrates with *S*-aryl *ortho*-substituents (Figure 3a). Similar Hammett ρ values of +0.49 and +0.53 were obtained, with the positive sign in each case consistent with an H/D-exchange process favoured by electron withdrawing X-substituents. By comparison with the reference acid dissociation of benzoin acids (ρ = +1.00, Figure 3b),[18] the sign of experimental ρ values determined herein can be aligned with a formal increase in electron density in the transition state for the rate-limiting step consistent with the formation of a neutral NHC from a cationic precursor. The smaller magnitude of ρ is unsurprising given the greater distance of the X-substituent from the site of deprotonation in *S*-triazolium ions versus the reference reaction (Figure 3b).

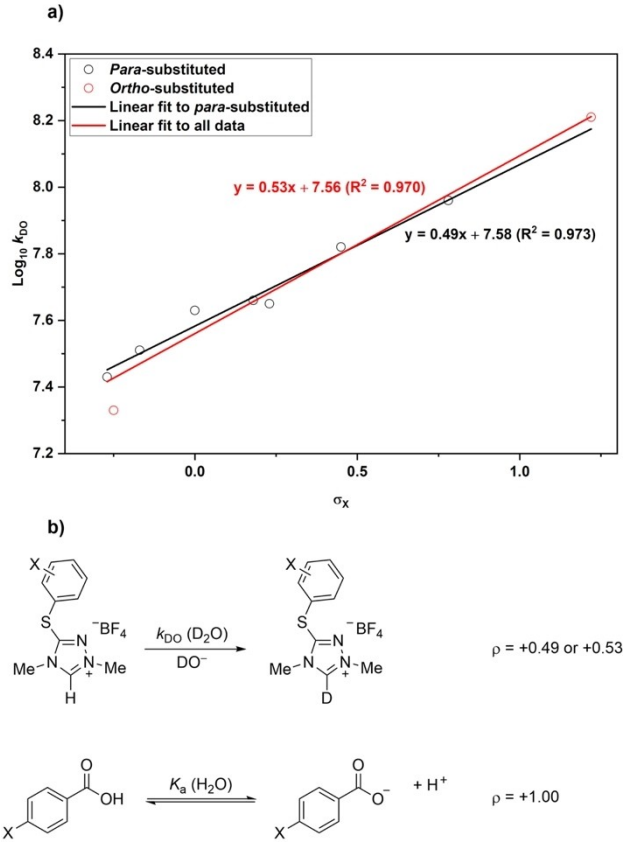

Figure 3. Hammett analysis of protofugality data: a) Hammett plots of Log_{10} k_{DO} versus substituent constant, σ_X; b) Comparison of the Hammett reaction constant ρ obtained in this work to the reference acid dissociation of *para*-substituted benzoic acids in water.

Hydrogen-deuterium exchange of the C(5)-hydrogen of isomeric 2,4-dimethyltriazolium salts **12** was substantially slower than for 1,4-isomers **5**. No significant change in ^{1}H NMR C(5)-H peak area was observed in methanol-d$_4$ for **12** on the same timescale for complete H/D-exchange for **5**. As the more acidic 'normal' NHC position between the *N*-alkylated nitrogen atoms is blocked by an S-aryl substituent in **12**, this observation is unsurprising and further ^{1}H NMR kinetic evaluation was not attempted owing to the long timescales required.

Structure-Protofugality Correlations

By analysis of XRD data, it is hoped relationships can be identified between specific structural parameters and experimental values of k_{DO}. Figure 4a assembles the ten single crystal X-ray structures obtained for the *S*-aryltriazolium series alongside Hammett σ_X and Log_{10} k_{DO} values. In all cases, the *S*-aryl ring is tilted relative to the central triazolium moiety. Table S24 and S25 collects dihedral angles, bond lengths and angles for each of the structures (ESI Section S4.1). Structural elements showing the strongest correlations to k_{DO} are illustrated in Figure 4b. The most dramatic changes are observed in dihedral angles D(C^3-S^6-C^7-C^9) and D(N^2-C^3-S^6-C^7) (°) with variation in the *S*-aryl moiety. Notably, reasonable linear correlations are observed between D(C^3-S^6-C^7-C^9) (°) and $\sigma_{p\text{-}X}$ (Figure S70, R^2 = 0.848) in addition to k_{DO} and D(C^3-S^6-C^7-C^9) (°) (Figure S71, R^2 = 0.778) with smaller dihedral angles aligning with higher $\sigma_{p\text{-}X}$ and k_{DO} values. Presumably more electron withdrawing *p*-substituents favour through-conjugation from sulfur towards the aryl substituent facilitated by increased co-planarity. By contrast, correlation of k_{DO} and | D(N^2-C^3-S^6-C^7) | (°) (Figure S72) is not linear but rather shows clustering of data around 25° and 100° respectively with a switch in dihedral angle occurring between σ_p = +0.23 (*p*-Br) and +0.45 (*p*-COOMe).

Decreases in k_{DO} values parallel lower C^3–S^6 and higher N^1–N^2 bond lengths (Figures S73, S74; R^2 = 0.818, 0.624). Greater conjugation from sulfur with the triazolium ring (lower C^3-S^6, Å) would be expected to attenuate cationic character and decrease protofugality as observed. Increasing distance from the carbenic position will decrease the electron withdrawing N^2 inductive effect also aligning with a lower k_{DO}. Attempted linear correlations of other parameters show substantially poorer overall fits. Notably, there was no significant change in the carbenic N^1-C^5-N^4 angle for all 1,4-dialkyltriazolium salts across the series **5 a-o·BF$_4$** (107.2-107.6°), however, this angle increases to 112° for 2,4-isomer **12 g.BF$_4$**.

Across the **5 a-o·BF$_4$** series there is a small but significant difference in each case between L(N^1–C^5) and L(N^4–C^5). For example, L(N^1–C^5) = 1.313 ±0.002 Å and L(N^4–C^5) = 1.335 ±0.002 Å for **5 a·BF$_4$**. The shorter L(N^1–C^5) bond lengths suggest more double bond character and greater conjugation from N^1

Research Article
doi.org/10.1002/ejoc.202400753

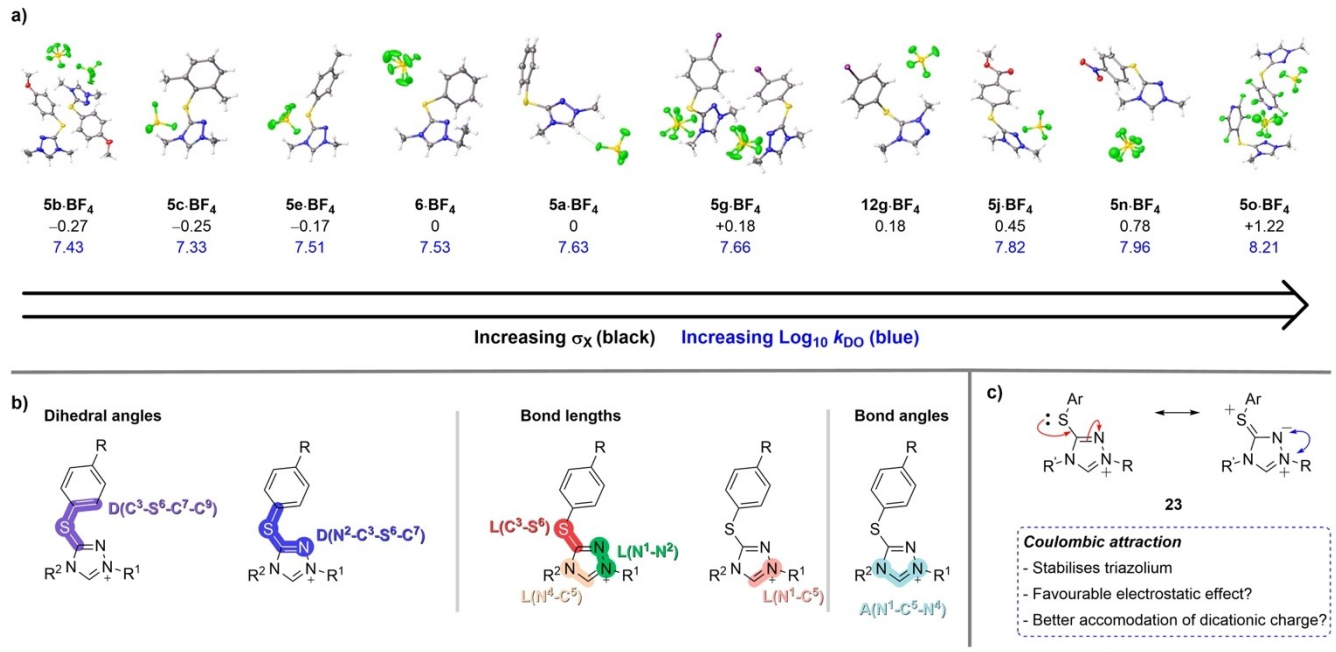

Figure 4. a) Summary of the 10 *S*-aryltriazolium salt single-crystal X-ray structures determined herein. X-ray structures are ordered based on the Hammett σ_X substituent constants of the *S*-aryl moiety and Log_{10} k_{DO} values. b) Summary of the XRD structural elements identified to show trends with σ_X and k_{DO}. c) The proposed role of coulombic attraction enabled by shorter L(N^1-C^5) and more cationic N^1.

to C^5 possibly allowing for greater dicationic charge stabilisation following sulfur-triazolium conjugation (**23**, Figure 4c). Multi-parameter fits were also explored using JMP software (for full details, see ESI Section S4.3). Fitting to Equation S13 was found to be the best model when including XRD data for all ten *S*-triazolium salts giving k_{DO} predictions with reasonable accuracy in comparison with experimental values

Determination of C(5)-H pK_a Values

The carbon acid pK_a values in water for the *S*-aryltriazolium salts may be estimated by application of Equation 6 derived for the acid dissociation in Equation 7. As discussed previously,[12] this kinetic approach may be used to estimate pK_a values in water when direct determination is precluded by the solvent levelling effect. As the conjugate acid pK_as of most NHC pre-catalysts are higher than for solvent water, quantitative deprotonation of solvent by NHC is favoured. The kinetic approach permits calculation of pK_a from the rate constants for the forward and reverse directions of the proton transfer equilibrium (Equation 6). In this equation, k_{HO} ($M^{-1}s^{-1}$) is the second order rate constant for deprotonation at C(5) by hydroxide ion, which may be calculated from the corresponding k_{DO} value using a value of $k_{DO}/k_{HO} = 2.4$ for the secondary solvent isotope effect on the basicity of HO^- in H_2O versus DO^- in D_2O. As discussed previously,[12] the absence of significant general base catalysis of deuterium exchange provides good evidence that the reverse protonation of the triazol-5-ylidene NHC by water is equal or close to the limiting rate constant for the physical process of dielectric relaxation of solvent ($k_{HOH} \leq k_{reorg} = 10^{11}\,s^{-1}$). By application of Equation 6, carbon acid pK_a values ranging from 16.9–18.6 could be calculated based on the protofugalities determined herein for the 11 triazolium salts **5 a-o·BF$_4$**, **6·BF$_4$** and **7·Br** (Table S23, ESI Section S3.5). In line with observations on protofugalities, these pK_a values are comparable to those determined for commonly used 1,2,4-triazolium organocatalysts and substantially lower than for related imidazolium NHC pre-catalysts.

$$pK_a = pK_w + \log\frac{k_{HOH}}{k_{HO}} \quad (6)$$

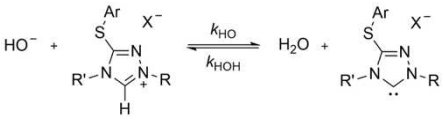

(7)

Conclusions

In summary, a large series of novel *N*, *N*-dialkyl 3-*S*-aryl-triazolium salts have been prepared from neutral triazole precursors. Methyl Cation Affinities (MCAs) of the neutral triazoles were determined computationally and found to agree with the experimental preference for N(1) over N(2)-methylation. Detailed kinetic proton transfer studies were undertaken by ^{1}H NMR spectroscopy permitting determination of first and second order rate constants (k_{ex} (s^{-1}) and k_{DO} ($M^{-1}s^{-1}$), respectively) for hydrogen-deuterium exchange at the C(5) pre-carbenic position for 11 *S*-aryltriazolium salts. Comparison of k_{DO} values (protofugalities towards conjugate base of water) across

the series enabled construction of a Protofugality Scale for ranking of relative kinetic acidities versus other common NHC pre-catalyst scaffolds. Specifically, the acidifying effect of an *S*-aryl substituent at C(3) results in similar protofugalities for **5 a-o·BF$_4$**, **6·BF$_4$** and **7·Br** compared to commonly used *N*-aryl-1,2,4-triazolium organocatalysts despite the former having two electron donating *N*-alkyl substituents that typically decrease protofugality. This highlights the benefit of distal exocyclic *S*-aryl substitution towards increasing NHC pre-catalyst acidity without needing more proximal *N*-aryl modification. Single crystal X-ray diffraction data were obtained for six *S*-aryltriazoles and ten *S*-aryltriazolium salts permitting detailed structural analysis and structure-protofugality correlations. Finally aqueous C(5)-H pK_as for the *S*-aryltriazolium salts could be calculated using experimental k_{DO} values.

Supporting Information Summary

The authors have cited additional references within the Supporting Information.[19]

Deposition Number CCDC 2366204–2366212, 2366219 (for *S*-aryl triazolium tetrafluoroborate salts **5 a**, **b**, **c**, **e**, **g**, **j**, **n**, **o.BF$_4$**, **6.BF$_4$**, **12 g.BF$_4$**), CCDC 2366213–2366218 (for *S*-aryl triazoles **9 a**, **e**, **i**, **j**, **n**, **o**), CCDC2366220 (for triazole **15**) contain(s) the supplementary crystallographic data for this paper. These data are provided free of charge by the joint Cambridge Crystallographic Data Centre and Fachinformationszentrum Karlsruhe Access Structures service.

Acknowledgements

The authors thank Durham University solution state NMR spectroscopy service, Durham University X-ray diffraction service and EPSRC (EP/S022791/1) for funding (MSS PhD studentship).

Conflict of Interests

The authors declare no conflict of interest.

Data Availability Statement

The data that support the findings of this study are available in the supplementary material of this article.

Keywords: N-Heterocyclic carbene · 1,2,4-Triazolium · Acidity · Sulfur substitution · Hammett analysis

[1] a) P. Bellotti, M. Koy, M. N. Hopkinson, F. Glorius, *Nat. Rev. Chem.* **2021**, *5*, 711–725; b) C. A. Smith, M. R. Narouz, P. A. Lummis, I. Singh, A. Nazemi, C.-H. Li, C. M. Crudden, *Chem. Rev.* **2019**, *119*, 4986–5056; c) E. Peris, *Chem. Rev.* **2018**, *118*, 9988–10031; d) D. M. Flanigan, F. Romanov-Michailidis, N. A. White, T. Rovis, *Chem. Rev.* **2015**, *115*, 9307–9387; e) K. M. Hindi, M. J. Panzner, C. A. Tessier, C. L. Cannon, W. J. Youngs, *Chem. Rev.* **2009**, *109*, 3859–3884.
[2] J. Rehbein, S.-M. Ruser, J. Phan, *Chem. Sci* **2015**, *6*, 6013–6018.
[3] a) M. P. van der Helm, B. Klemm, R. Eelkema, *Nat. Rev. Chem.* **2019**, *3*, 491–508; b) J. Yan, R. Sun, K. Shi, K. Li, L. Yang, G. Zhong, *J. Org. Chem* **2018**, *83*, 7547–7552.
[4] D. Enders, O. Niemeier, A. Henseler, *Chem. Rev.* **2007**, *107*, 5606–5655.
[5] a) V. I. Bunik, A. Tylicki, N. V. Lukashev, *FEBS J* **2013**, *280*, 6412–6442; b) F. Jordan, N. S. Nemeria, A. Balakrishnan, J. Chakraborty, E. Guevara, P. Nareddy, H. Patel, D. J. Shim, J. Wang, L. Yang, X. Zhang, J. Zhou, *4.05 – An Update on Developments in the Field of Thiamin Diphosphate-Dependent Enzymes.* In Comprehensive Natural Products III (Eds.: H.-W. Liu, T. P. Begley), Elsevier, Oxford, **2020**, pp. 58–110; c) T. Sehl, S. Bock, L. Marx, Z. Maugeri, L. Walter, R. Westphal, C. Vogel, U. Menyes, M. Erhardt, M. Müller, M. Pohl, D. Rother, *Green Chem.* **2017**, *19*, 380–384; d) M. Müller, G. A. Sprenger, M. Pohl, *Curr. Opin. Chem. Biol.* **2013**, *17*, 261–270; e) J. C. Sheehan, D. H. Hunneman, *J. Am. Chem. Soc.* **1966**, *88*, 3666–3667; f) R. L. Knight, F. J. Leeper, *Tetrahedron Lett.* **1997**, *38*, 3611–3614; g) J. C. Sheehan, T. Hara, *J. Org. Chem* **1974**, *39*, 1196–1199.
[6] a) J. Song, J. Zou, J. Jin, J. Lv, C. Mou, Y. R. Chi, *Chem. Eur. J* **2023**, *29*, e202203661; b) W. Chen, X.-Y. Deng, Y. Li, L.-J. Yang, W.-C. Wan, X.-Q. Wang, H.-B. Zhang, X.-D. Yang, *Bioorg. Med. Chem. Lett.* **2013**, *23*, 4297–4302; c) X. Chen, Y. M. Shi, C. Huang, S. Xia, L. J. Yang, X. D. Yang, *Anticancer Agents Med Chem* **2016**, *16*, 377–386; d) Z. J. Lin, J. Bies, S. S. Johnson, J. D. Gorden, J. F. Strickland, M. Frazier, J. M. Meyers, K. L. Shelton, *J. Heterocycl. Chem.* **2019**, *56*, 533–538; e) P. L. McCormack, *Drugs* **2015**, *75*, 817–822; f) I. Pahuja, A. Verma, A. Ghoshal, S. Mukhopadhyay, A. Kumari, A. Shaji, S. Chaturvedi, V. P. Dwivedi, A. Bhaskar, *Microbiol. Spectr.* **2023**, *11*, e00858–00823; g) W. Lee, M.-C. Baek, K.-M. Kim, J.-S. Bae, *Int. J. Mol. Sci.* **2020**, *21*, 1462
[7] J. Clayden, N. Greeves, S. Warren, in *Organic Chemistry*, Second ed., (Eds.: J. Clayden, N. Greeves, S. Warren), Oxford University Press, Oxford, UK, **2012**, pp. 660–664.
[8] M. Numata, M. Yamaoka, I. Minamida, M. Kuritani, Y. Imashiro, *J Antibiot* **1978**, *31*, 1245–1251.
[9] H. Mayr, A. R. Ofial, *Acc. Chem. Res.* **2016**, *49*, 952–965.
[10] Protofugality describes the tendency for loss of a proton usually by proton transfer to a basic species For comparison of relative protofugalities, the same base should be employed. Herein, proton transfer to the conjugate base of solvent is kinetically assessed.
[11] N. Ree, A. H. Göller, J. H. Jensen, *Digital Discovery* **2024**, *3*, 347–354.
[12] a) J. Zhu, I. Moreno, P. Quinn, D. S. Yufit, L. Song, C. M. Young, Z. Duan, A. R. Tyler, P. G. Waddell, M. J. Hall, M. R. Probert, A. D. Smith, A. C. O'Donoghue, *J. Org. Chem* **2022**, *87*, 4241–4253; b) P. Quinn, M. S. Smith, J. Zhu, D. R. W. Hodgson, A. C. O'Donoghue, *Catalysts* **2021**, *11*, 1055; c) D. E. Tucker, P. Quinn, R. S. Massey, C. J. Collett, D. J. Jasiewicz, C. R. Bramley, A. D. Smith, A. C. O'Donoghue, *J. Phys. Org. Chem.* **2015**, *28*, 108–115; d) R. S. Massey, C. J. Collett, A. G. Lindsay, A. D. Smith, A. C. O'Donoghue, *J. Am. Chem. Soc.* **2012**, *134*, 20421–20432
[13] a) R. S. Massey, J. Murray, C. J. Collett, J. Zhu, A. D. Smith, A. C. O'Donoghue, *Org. Biomol. Chem* **2021**, *19*, 387–393; b) C. J. Collett, C. M. Young, R. S. Massey, A. C. O'Donoghue, A. D. Smith, *Eur. J. Org. Chem.* **2021**, *2021*, 3670–3675; c) C. J. Collett, R. S. Massey, J. E. Taylor, O. R. Maguire, A. C. O'Donoghue, A. D. Smith, *Angew. Chem. Int. Ed.* **2015**, *54*, 6887–6892; d) C. J. Collett, R. S. Massey, O. R. Maguire, A. S. Batsanov, A. C. O'Donoghue, A. D. Smith, *Chem. Sci* **2013**, *4*, 1514–1522; e) T. L. Amyes, S. T. Diver, J. P. Richard, F. M. Rivas, K. Toth, *J. Am. Chem. Soc.* **2004**, *126*, 4366–4374; f) J. T. Stivers, M. W. Washabaugh, *Bioorg. Chem.* **1992**, *20*, 155–172; g) M. W. Washabaugh, W. P. Jencks, *J. Am. Chem. Soc.* **1989**, *111*, 683–692; h) M. W. Washabaugh, W. P. Jencks, *Biochem.* **1988**, *27*, 5044–5053; i) G. Gish, T. Smyth, R. Kluger, *J. Am. Chem. Soc.* **1988**, *110*, 6230–6234; j) R. Kluger, *Chem. Rev.* **1987**, *87*, 863–876; k) D. S. Kemp, J. T. O'Brien, *J. Am. Chem. Soc.* **1970**, *92*, 2554–2555; l) J. Crosby, G. E. Lienhard, *J. Am. Chem. Soc.* **1970**, *92*, 5707–5716; m) R. Breslow, *Ann. N. Y. Acad. Sci.* **1962**, *98*, 445–452
[14] C. Hansch, A. Leo, R. W. Taft, *Chem. Rev.* **1991**, *91*, 165–195.
[15] A. K. Covington, R. A. Robinson, R. G. Bates, *J. Phys. Chem.* **1966**, *70*, 3820–3824.
[16] K. Maduka, PhD thesis, Durham University (UK), **2019**.
[17] E. M. Higgins, J. A. Sherwood, A. G. Lindsay, J. Armstrong, R. S. Massey, R. W. Alder, A. C. O'Donoghue, *Chem. Commun.* **2011**, *47*, 1559–1561.
[18] L. P. Hammett, *J. Am. Chem. Soc.* **1937**, *59*, 96–103.
[19] a) O. V. Dolomanov, L. J. Bourhis, R. J. Gildea, J. A. K. Howard, H. Puschmann, *J. Appl. Crystallogr.* **2009**, *42*, 339–341; b) G. M. Sheldrick, *Acta Crystallogr. Sect. A: Found. Crystallogr.* **2015**, *71*, 3–8; c) J. C. Antilla,

J. M. Baskin, T. E. Barder, S. L. Buchwald, *J. Org. Chem* **2004**, *69*, 5578–5587; d) P. K. Glasoe, F. A. Long, *J. Phys. Chem.* **1960**, *64*, 188–190; e) L. G. Gagliardi, C. B. Castells, C. Ràfols, M. Rosés, E. Bosch, *Anal. Chem.* **2007**, *79*, 3180–3187; f) H. S. Harned, R. A. Robinson, *Trans. Faraday Soc.* **1940**, *36*, 973–978; g) M. Roses, C. Rafols, E. Bosch, *Anal. Chem.* **1993**, *65*, 2294–2299; h) J. K. Barral, E. Gudmundson, N. Stikov, M. Etezadi-Amoli, P. Stoica, D. G. Nishimura, *Magn. Reson. Med.* **2010**, *64*, 1057–1067; i) M. Charton, *Can. J. Chem.* **1960**, *38*, 2493–2499; j) A. J. Kresge, R. A. M. O'Ferrall, M. F. Powell, in *Isotopes in organic chemistry* (Eds.: E. Buncel, C. C. Lee), Elsevier, New York, **1977**; k) R. S. Massey, P. Quinn, S. Zhou, J. A. Murphy, A. C. O'Donoghue, *J. Phys. Org. Chem.* **2016**, *29*, 735–740; l) L. Baragwanath, C. A. Rose, K. Zeitler, S. J. Connon, *J. Org. Chem* **2009**, *74*, 9214–9217; m) U. Kaatze, *J. Chem. Eng. Data* **1989**, *34*, 371–374

Manuscript received: July 3, 2024
Revised manuscript received: August 30, 2024
Accepted manuscript online: September 16, 2024
Version of record online: ■■, ■■

RESEARCH ARTICLE

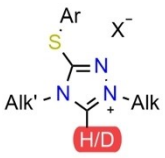

- Synthesis of large series of novel 1,4-dialkyl *S*-aryltriazolium ions
- C(5) H/D exchange – **protofugality scale**
- Hammett analysis upon Ar: ρ = 0.53
- XRD analysis and correlation to C(5) H/D exchange

Acidifying effect of distal C(3)-sulfur on C(5)-H
Allows for two N-alkyl substituents whilst maintaining acidity

*M. S. Smith, T. J. Blundell, I. Hickson, A. C. O'Donoghue**

S-Aryl Substitution Enhances Acidity of the 1,2,4-Triazolium Scaffold

A large series of novel N,N-dialkyl-1,2,4-triazolium salts with 3-S-aryl substituents was prepared from neutral S-aryl triazole precursors. High protofugalities (kinetic acidities) were demonstrated for C(5)-H highlighting the acidifying effect of the distal C(3)-sulfur with mechanistic insight obtained from XRD-protofugality correlations.